

Supplemental Information

Approved Anti-Cancer Drugs Target Oncogenic Non-Coding RNAs

Sai Pradeep Velagapudi¹, Matthew G. Costales¹, Balayeshwanth R. Vummidi¹, Yoshio Nakai¹, Alicia J. Angelbello¹, Tuan Tran¹, Hafeez S. Haniff¹, Yasumasa Matsumoto¹, Zi Fu Wang¹, Arnab K. Chatterjee², Jessica L. Childs-Disney¹, and Matthew D. Disney^{1,3,*}

¹Department of Chemistry, The Scripps Research Institute, 130 Scripps Way, Jupiter, FL 33458

²California Institute for Biomedical Research (CALIBR), 11119 North Torrey Pines Road, Suite 100, La Jolla, CA 92037

³Lead Contact

*Correspondence: Disney@scripps.edu (M.D.D.)

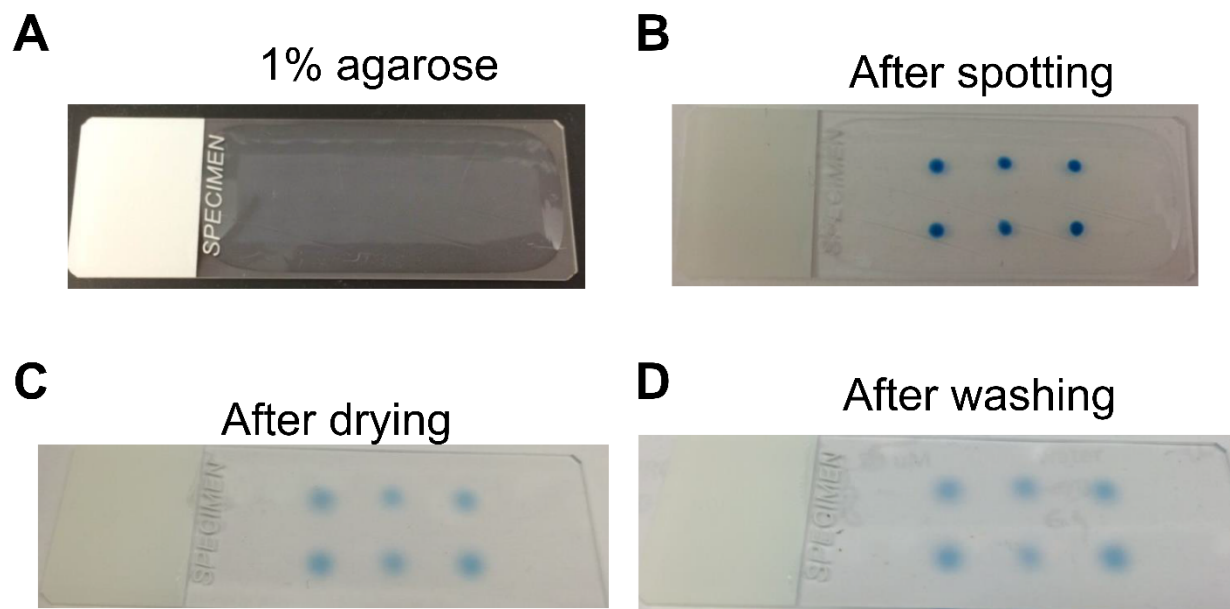


Figure S1: AbsorbArray slide construction. Related to Figure 1. **A**, image of 1% agarose slide [Fisher Scientific, 12550016; 75 x 25 x 1 mm (width x height x thickness)]. **B**, image of a glass slide after spotting compound **3** into agarose gel surface. **C**, image of slide pinned with compound **3** after drying agarose into a thin film. **D**, image of slide after washing.

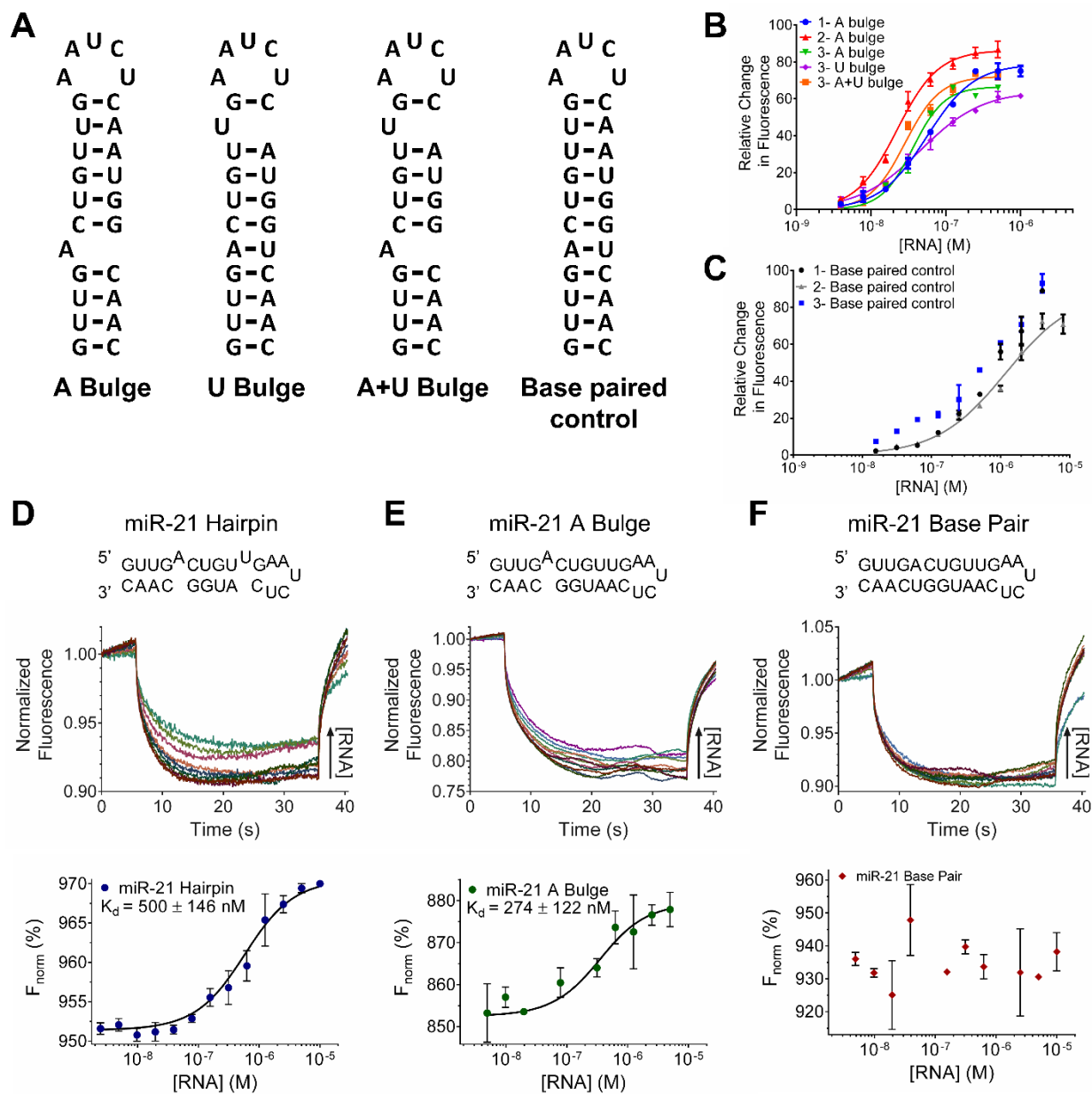


Figure S2: Binding affinities of compounds to the A and U bulges in the miR-21 hairpin precursor. Related to Figure 2 and Table 2. A, secondary structures of A bulge, U bulge, A+U bulge, and base-paired control used for studying binding affinities of topoisomerase inhibitors by fluorescence. **B**, representative fluorescent binding isotherms of compounds **1**, **2**, and **3** to RNAs containing an A bulge, U bulge, or an A+U bulge. **C**, representative fluorescent binding isotherms of compounds **1**, **2**, and **3** to a base-paired control RNA. **D**, microscale thermophoresis (MST) binding analyses of compound **3** to a RNA construct containing both the A and U bulge displayed

in the miR-21 hairpin precursor (miR-21 Hairpin Full); **E**, a RNA construct containing only the A bulge displayed in the miR-21 hairpin precursor (miR-21 A Bulge), and; **F**, a base paired control RNA construct (miR-21 Base Pair). Data represents mean \pm s.d.

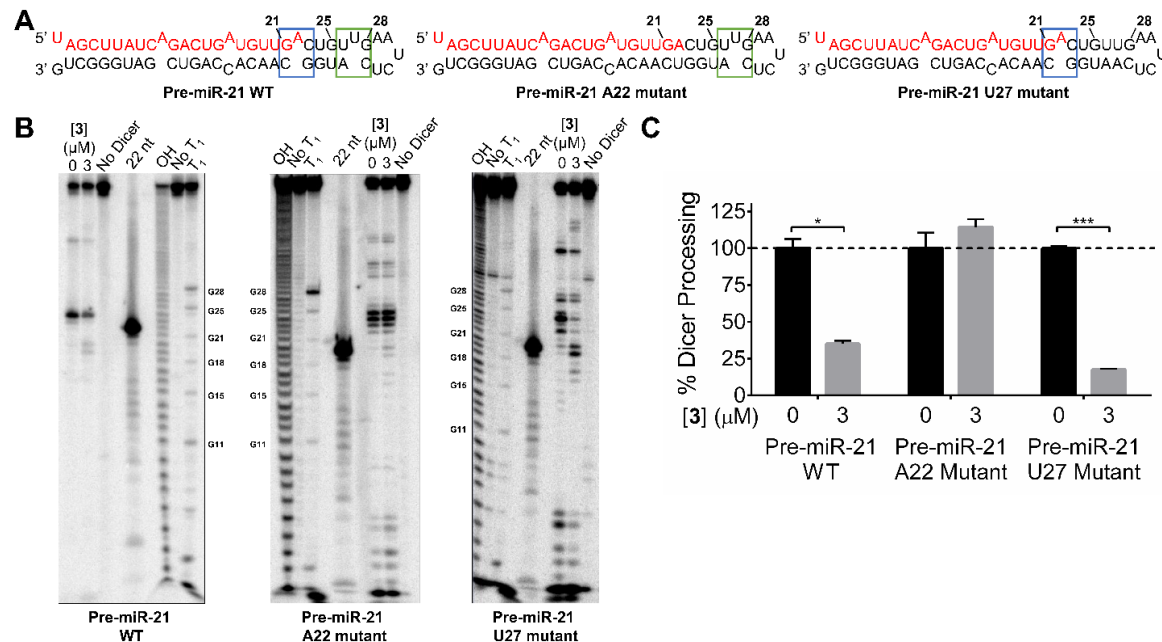


Figure S3: *In vitro* Dicer processing of pre-miR-21 wild type and pre-miR-21 A22 mutant.

Related to Figure 2. **A**, pre-miR-21 RNA constructs used in this study. Pre-miR-21 A22 Mutant is the same as the Pre-miR-21 WT, but with the A bulge base paired to a U. Pre-miR-21 U27 Mutant is the same as Pre-miR-21 WT, but with the U bulge base paired to an A. Blue boxes represent A bulge binding site, green boxes represent U bulge binding site, and red text represents mature miR-21 product. **B**, Representative gels of *in vitro* Dicer processing of Pre-miR-21 WT and Pre-miR-21 A22 mutant with compound **3**. **C**, quantification of the Dicer processing bands shown in **B**. Data represents mean \pm s.e.m. ($n \geq 3$). * indicates $p < 0.5$; *** indicates $p < 0.001$, as determined by a two-tailed student t test.

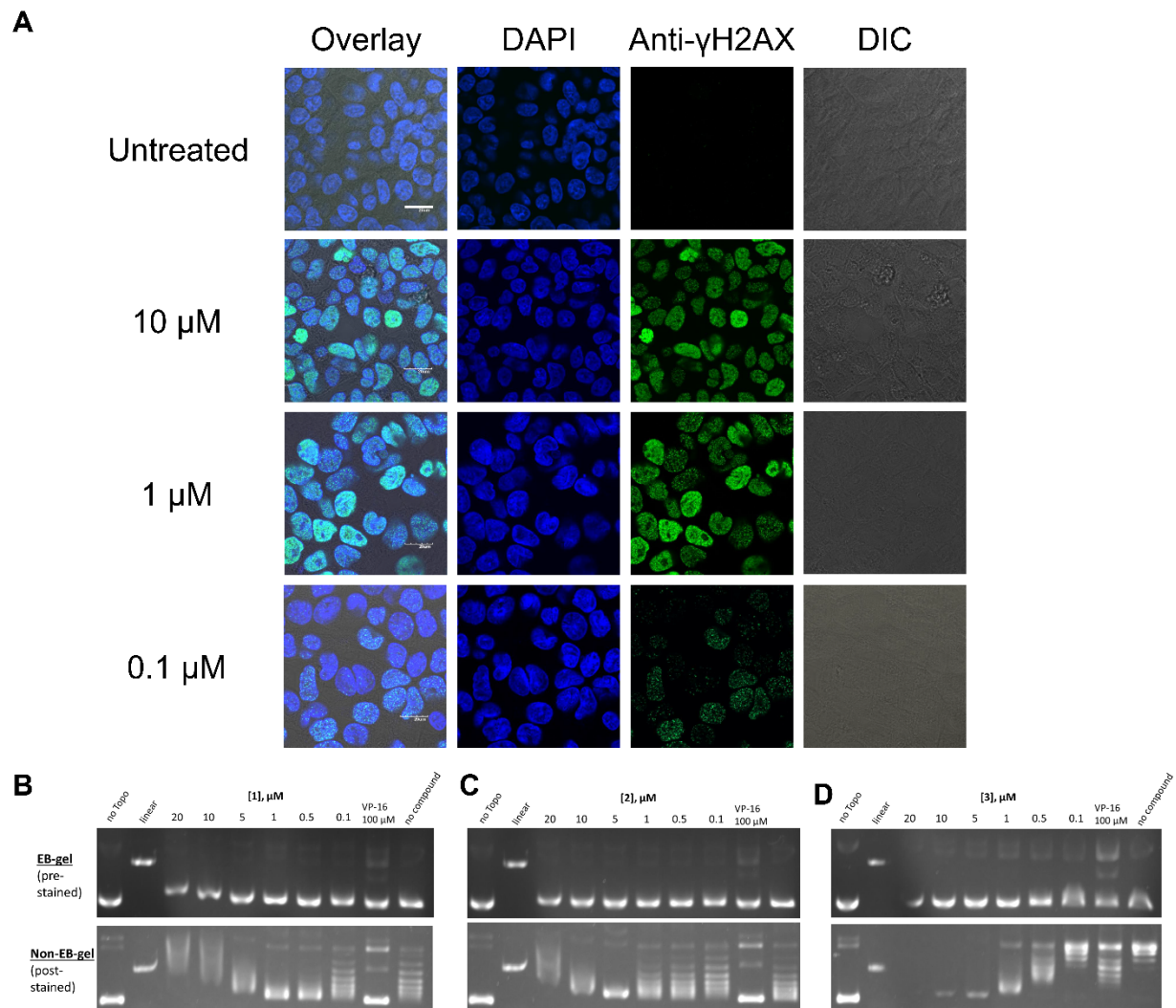


Figure S4: Effect of compounds on DNA damage in MDA-MB-231 cells. Related to Figure 3. **A**, representative images of DNA damage resulting from **3** treatment, as analyzed by staining for γ -H2AX foci. **B**, the effect of topoisomerase inhibitor compounds on topoisomerase activity as analyzed by an *in vitro* topoisomerase inhibition assay.

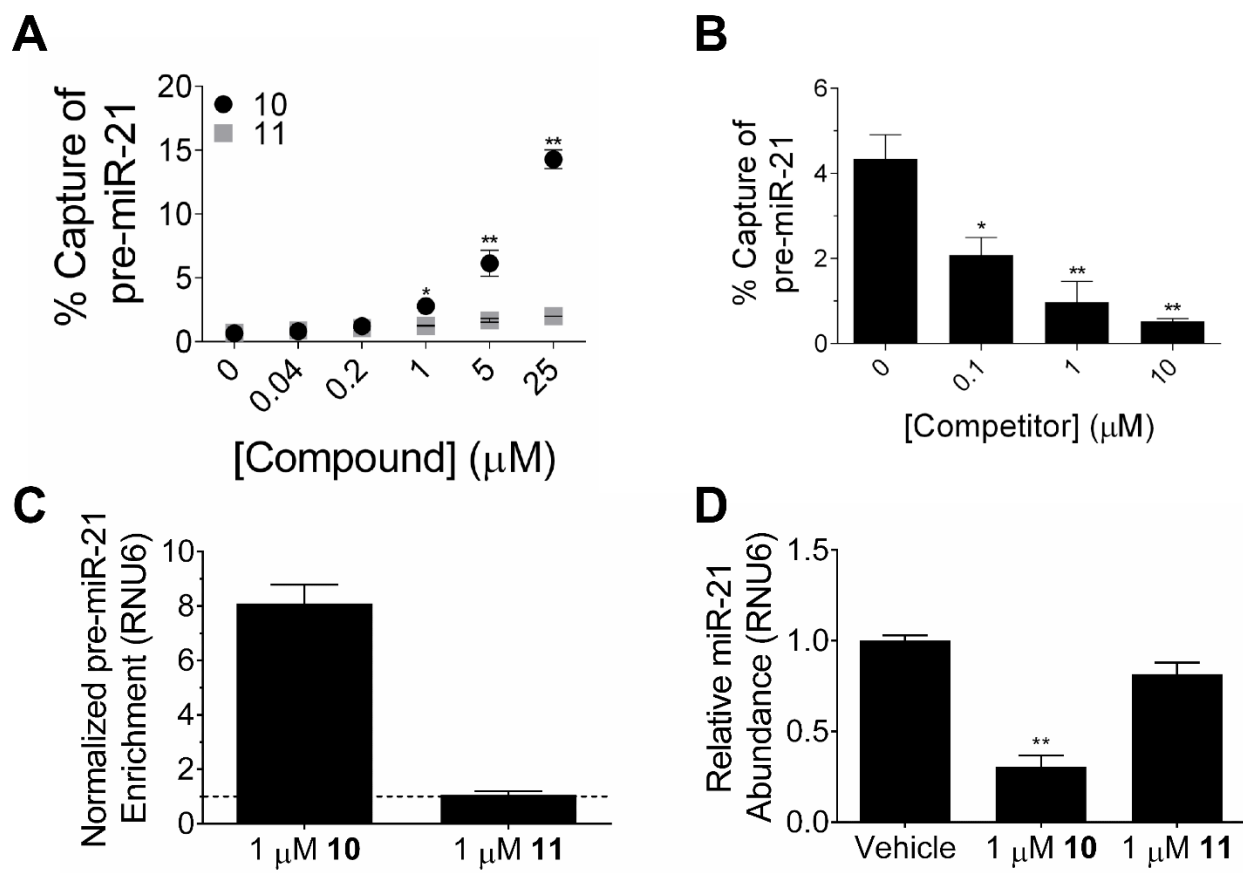


Figure S5: Small molecule target validation in vitro and effects of Chem-CLIP compounds 10 and 11 in cells. Related to Figure 4. A, in vitro Chem-CLIP of pre-miR-21. * indicates $p < 0.5$; ** indicates $p < 0.01$, when comparing percent capture by compound 10 to percent capture by compound 11, as determined by a two-tailed student t test. **B**, in vitro C-Chem-CLIP of pre-miR-21 by using increasing concentrations of 3 to compete with 10 for binding (1 μM). * indicates $p < 0.5$; ** indicates $p < 0.01$, when comparing percent capture with and without competitor, as determined by a two-tailed student t test. **C**, Chem-CLIP of pre-miR-21 using 1 μM of 10 and 11 in MDA-MB-231 cells. **D**, mature miR-21 biogenesis is inhibited at 1 μM of 10. ** indicates $p < 0.01$, when comparing treated to vehicle samples, as determined by a two-tailed student t test.

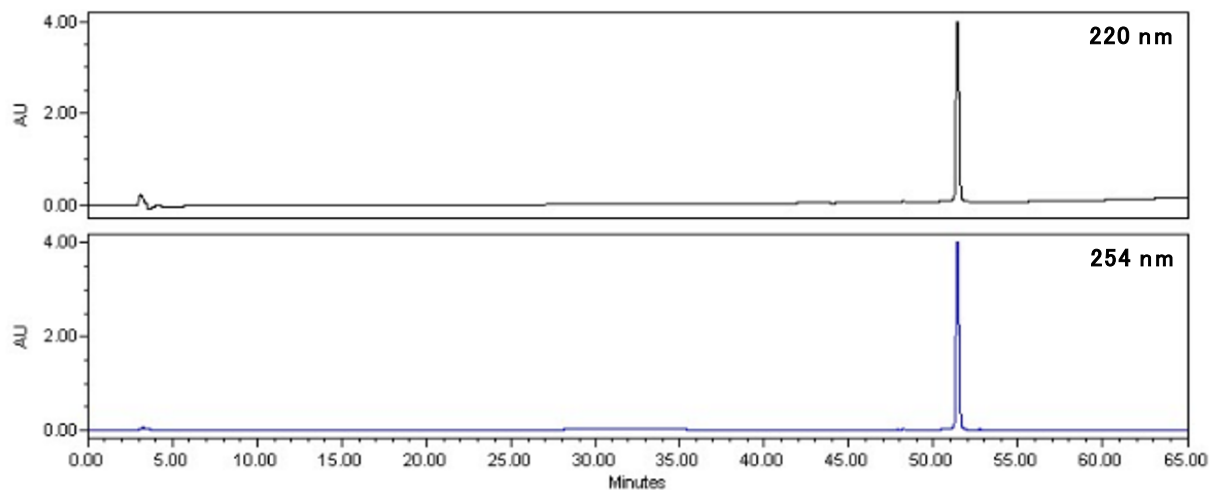


Figure S6: Analytical HPLC trace of 10. Related to STAR Methods. A linear gradient with a flow rate of 1 mL/min from 0% to 100% acetonitrile in H₂O with 0.1% (v/v) TFA over 60 min was used.

Table S1: Inforna search identifies topoisomerase inhibitors 2 and 3 can target miRNAs that are upregulated in cancers with high fitness score (>50). Related to Table 1.

Small Molecule	Target Site	miRNA	Drosha/Dicer	Cancer
2	5'CAG/3'CG	hsa-miR-21	Dicer	multiple cancers
3	5'GCC/3'AU	hsa-miR-487a	Dicer	breast and liver
3	5'GCC/3'AUU	hsa-miR-106a	Dicer	multiple cancers
3	5'UUA/3'CG	hsa-miR-25	Dicer	multiple cancers
3	5'GCC/3'AAU	hsa-miR-23a	Drosha	breast and lung
3	5'AGU/3'CGG	hsa-miR-661	Drosha	breast
3	5'AGU/3'CGG	hsa-miR-27a	Dicer	breast
3	5'CAG/3'CG	hsa-miR-21	Dicer	multiple cancers
3	5'UUA/3'CG	hsa-miR-21	Adjacent to Dicer	multiple cancers

Table S2: Sequences of primers used for RT-qPCR. Related to STAR Methods.	
hsa-miR-21	TAGCTTATCAGACTGATGTTGA
let-7e	TGAGGTAGGAGGTTGTATAGTT
hsa-miR-25	CATTGCACTTGTCTCGGTCTGA
hsa-miR-181b-2	AACATTCATTGCTGTCGGTGGGT
hsa-miR-449a	TGGCAGTGTATTGTTAGCTGGT
hsa-miR-555	AGGGTAAGCTGAACCTCTGAT
hsa-miR-3130	GCTGCACCGGAGACTGGGTAA
hsa-miR-3616	CGAGGGCATTTCATGATGCAGGC
hsa-miR-4739	AAGGGAGGAGGAGCGGAGGGGCCCT
hsa-miR-4673	TCCAGGCAGGAGCCGGACTGGA
RNU6	ACACGCAAATTCGTGAAGCGTTC
Universal Reverse	GAATCGAGCACCAGTTACGC
18S-F	GTAACCCGTTGAACCCATT
18S-R	CCATCCAATCGGTAGTAGCG
hsa-pre-miR-21-F	CTGATGTTGACTGTTGAATC
hsa-pre-miR-21-R	GCCCATCGACTGGTGTGTC